Charge-distribution effect of imaging molecular structure by high-order above-threshold ionization

Bingbing Wang,[1,*] Yingchun Guo,[2,†] Bin Zhang,[3] Zengxiu Zhao,[3] Zong-Chao Yan,[4] and Panming Fu[1]

[1]*Laboratory of Optical Physics, Beijing National Laboratory for Condensed Matter Physics, Institute of Physics, Chinese Academy of Sciences, Beijing 100080, China*

[2]*Department of Physics, State Key Laboratory of Precision Spectroscopy, East China Normal University, Shanghai 200062, China*

[3]*Department of Physics, National University of Defense Technology, Changsha 410073, China*

[4]*Department of Physics, University of New Brunswick, Fredericton, New Brunswick E3B 5A3, Canada*

(Received 28 April 2010; published 5 October 2010)

Using a triatomic molecular model, we show that the interference pattern in the high-order above-threshold ionization (HATI) spectrum depends dramatically on the charge distribution of the molecular ion. Therefore the charge distribution can be considered a crucial factor for imaging a molecular geometric structure. Based on this study, a general destructive interference formula for each above-threshold ionization channel is obtained for a polyatomic molecule concerning the positions and charge values of each nuclei. Comparisons are made for the HATI spectra of CO_2, O_2, NO_2, and N_2. These results may shed light on imaging complex molecular structure by the HATI spectrum.

DOI: 10.1103/PhysRevA.82.043402 PACS number(s): 32.80.Rm, 42.65.−k, 42.50.Hz

I. INTRODUCTION

The recollision process of an ionized electron driven by a laser field provides a novel tool for investigating the internal characteristics of an atom [1–4] or a molecule [5–14]. High-order harmonic generation (HHG) and high-order above-threshold ionization (HATI) are two ideal processes for achieving this purpose [15]. In a recollision process, first an electron is ionized by a laser field, then it is driven by the laser and oscillates, and finally, it returns to the parent ion, resulting in either recombination to the ground state and emission of a harmonic photon or elastic collision with the ion [16]. Based on the concept of recollision, although the outermost electron's orbital and the geometric structure of a molecule can both leave a fingerprint on the HATI or HHG spectrum, HATI can be regarded as a more direct way to image molecular geometric structure. This is because the last step in HATI is an elastic potential scattering process, which is closely connected with the geometric structure of the molecule, while HHG is a suitable process for imaging a molecular orbital due to the recombination nature of the plane wave of the ionized electron to the ground state of the molecule, under the strong-field approximation.

In this work, we study the HATI of a molecule by using the frequency-domain theory based on the nonperturbative quantum electrodynamics approach, which was first developed by Guo *et al.* [17]. Recently, this method was successfully extended to deal with HHG [18,19] and HATI [20–22]. Especially, Fu *et al.* established the relationship between the frequency-domain theory and the time-domain theory in strong-field physics [19], and they discussed the difference and correspondence between the frequency- and the time-domain picture of the HATI process [20]. In the frequency-domain picture, the dynamics of the HATI process can be understood as a two-step transition: an above-threshhold ionization (ATI) followed by a laser-assisted collision (LAC).

As we showed in our recent paper [21], the interference pattern in a HATI spectrum comes from three sources: the wave function of the initial state, the geometric structure of the molecule, and the oscillation of the recollision electron. The interference by an oscillating electron exists in all HATI spectra, no matter what kind of target it is: an atom or a molecule. For a homonuclear diatomic molecule, additional interference fringes appear because it involves a two-center recollision process [5]. Recently, the dependence of interference fringes of a HATI spectrum on molecular structure has been studied theoretically [23–28] and experimentally [22,29]. Especially, Busuladzic *et al.* have found that the minima of the ionization rate of N_2 obey the relation $E_f \cos^2\theta = \pi^2/(2R_0^2)$ for a perpendicular orientation, where E_f is the electron kinetic energy, θ the electron emission angle, and R_0 the internuclear distance.

In this paper, we demonstrate that imaging of the geometric structure of a heteronuclear molecule by the HATI spectrum strongly depends on the charge distribution of the corresponding molecular ion. When an active electron is ionized by a laser field, the remaining electrons in the molecular ion will rearrange their distribution around the nuclei and thus different nuclei will carry different charge values. Therefore, the recollision electron will feel different attractive forces from the different nuclei when it returns. As a result, the final HATI spectrum will be affected by the charge distribution of the molecular ion and the interference fringes on the HATI spectrum will show a strong dependence on this charge distribution.

This paper is organized as follows. In Sec. II, we briefly review the basics of the frequency-domain theory of the HATI process. In Sec. III, we investigate the relationship between a HATI spectrum and the charge distribution in an *A*-*B*-*A* model molecule. Furthermore, we develop a general formula for each ATI channel regarding destructive interference fringes in a HATI spectrum for a molecule of an arbitrary number of

*wbb@aphy.iphy.ac.cn
†ycguo@phy.ecnu.edu.cn

atoms. In Sec. IV, we compare HATI spectra of O_2, CO_2, NO_2, and N_2 molecules. Finally, in Sec. V, we give our conclusions.

II. FREQUENCY-DOMAIN THEORY

The frequency-domain representation of the theory for HATI in a strong laser field is described in detail in [20]. Here we briefly summarize the basic elements of this theory and the modifications for a triatomic molecular system. Atomic units are used throughout unless stated otherwise. The Hamiltonian for a molecule-laser system is

$$H = H_0 + U(\mathbf{r}) + V, \tag{1}$$

where

$$H_0 = \frac{(-i\nabla)^2}{2m_e} + \omega N_a \tag{2}$$

is the energy operator for a free electron-photon system, $N_a = (a^\dagger a + aa^\dagger)/2$ is the photon number operator, with a ($a^\dagger$) being the annihilation (creation) operator of the laser photon mode, $U(\mathbf{r})$ is the molecular binding potential, which characterizes the geometry structure of the molecule, and V is the electron-photon interaction

$$V = -\frac{e}{m_e}\mathbf{A}(\mathbf{r})\cdot(-i\nabla) + \frac{e^2\mathbf{A}^2(\mathbf{r})}{2m_e}, \tag{3}$$

with e being the electron charge, and thus $e<0$, $\mathbf{A}(\mathbf{r}) = g(\hat{\boldsymbol{\epsilon}}\, a\, e^{i\mathbf{k}\cdot\mathbf{r}} + \text{c.c.})$ being the vector potential, $g = (2\omega V_e)^{-1/2}$, V_e the normalization volume of the field, and $\hat{\boldsymbol{\epsilon}}$ the polarization vector of the laser photon mode.

The time-independent feature of the field-quantized Hamiltonian enables us to treat HATI as a genuine scattering process in an isolated system that consists of photons and a molecule. The transition matrix element can be written as

$$T_{fi} = \langle\psi_f|V|\psi_i\rangle + \langle\psi_f|U\frac{1}{E_f - H + i\varepsilon}V|\psi_i\rangle, \tag{4}$$

where the initial state $|\psi_i\rangle = |\Phi_i(\mathbf{r}),n_i\rangle = \Phi_i(\mathbf{r})\otimes|n_i\rangle$ is the eigenstate of the Hamiltonian $H_0 + U(\mathbf{r})$ with the associated energy $E_i = -E_B + (n_i + \frac{1}{2})\omega$. Furthermore, $\Phi_i(\mathbf{r})$ is the ground-state wave function of the molecule with the binding energy E_B and $|n_i\rangle$ is the Fock state of the laser mode with photon number n_i. In contrast, the final state $|\psi_f\rangle = |\Psi_{\mathbf{p}_f n_f}\rangle$ of energy $E_f = E_{\mathbf{p}_f n_f}$ is a Volkov state of the quantized field [17,30].

The first and second terms in Eq. (4) correspond to the processes of direct and rescattering ATI, respectively. Thus, T_{fi} can be expressed as $T_{fi} = T_\mathrm{d} + T_\mathrm{r}$, where the direct ATI transition is $T_\mathrm{d} = \langle\psi_f|V|\psi_i\rangle$ and the rescattering ATI transition is

$$\begin{aligned} T_\mathrm{r} &= -i\pi\sum_{\mathbf{p}_1 n_1}\langle\Psi_{\mathbf{p}_f n_f}|U|\Psi_{\mathbf{p}_1 n_1}\rangle\langle\Psi_{\mathbf{p}_1 n_1}|V|\Phi_i,n_i\rangle\delta(E_f - E_{\mathbf{p}_1 n_1}) \\ &= -i\pi\sum_{\text{all channels}} T_\mathrm{LAC}T_\mathrm{ATI}\,\delta(E_f - E_{\mathbf{p}_1 n_1}). \end{aligned} \tag{5}$$

To obtain Eq. (5), we have used the completeness relation of the Volkov states $|\Psi_{\mathbf{p}_1 n_1}\rangle$ and the strong-field approximation; that is, the binding potential U can be neglected when the electron is in the continuum. The physics underlying Eq. (5) is clear. Specifically, $T_\mathrm{ATI} = \langle\Psi_{\mathbf{p}_1 n_1}|V|\Phi_i,n_i\rangle$ represents the direct ATI amplitude, where the ground-state electron absorbs $n_i - n_1$ photons from the laser field and ionizes, whereas $T_\mathrm{LAC} = \langle\Psi_{\mathbf{p}_f n_f}|U|\Psi_{\mathbf{p}_1 n_1}\rangle$ represents the amplitude of an LAC in which the ionized electron absorbs $n_1 - n_f$ photons from the field during its collision with the nucleus. As a result, the canonical momentum of the electron changes from $\mathbf{p}_1$ to $\mathbf{p}_f$. Therefore, from the frequency-domain viewpoint, the recollision ATI can be described simply as an ATI followed by an LAC with all ATI channels summed up coherently.

Using Eq. (3), the ATI transition can be written as [17,30]

$$\begin{aligned} T_\mathrm{ATI} &= \langle\Psi_{\mathbf{p}_1 n_1}|V|\Phi_i,n_i\rangle \\ &= V_e^{-1/2}\omega(u_p - j)\Phi(\mathbf{p}_1)\mathcal{J}_j(\zeta_1,\eta,\phi_\xi), \end{aligned} \tag{6}$$

where $j = n_i - n_1$, the generalized Bessel functions $\mathcal{J}_j(\zeta_1,\eta,\phi_\xi) = \sum_{m=-\infty}^{\infty} J_{-j-2m}(\zeta_1)J_m(\eta)e^{i2m\phi_\xi}$, with $\zeta_1 = \sqrt{2u_p/\omega}\,\mathbf{p}_1\cdot\hat{\boldsymbol{\epsilon}}$, $\eta = u_p/2$, and $\phi_\xi = \tan^{-1}(p_{1y}/p_{1x})$. Furthermore, $u_p = U_p/\omega$, with U_p being the ponderomotive energy of an electron in the laser field, and $\Phi(\mathbf{p}_1)$ is the Fourier transform of the initial wave function $\Phi_i(\mathbf{r})$. In contrast, the transition matrix element of an LAC can be written as

$$\begin{aligned} T_\mathrm{LAC} &= \langle\Psi_{\mathbf{p}_f n_f}|U|\Psi_{\mathbf{p}_1 n_1}\rangle \\ &= V_e^{-1}J_s(\zeta_1 - \zeta_f)\langle\mathbf{p}_f|U|\mathbf{p}_1\rangle, \end{aligned} \tag{7}$$

where $s = n_1 - n_f$, $\zeta_f = \sqrt{2u_p/\omega}\,\mathbf{p}_f\cdot\hat{\boldsymbol{\epsilon}}$, and $\langle\mathbf{p}_f|U|\mathbf{p}_1\rangle = \int d^3\mathbf{r}\exp[-i(\mathbf{p}_f - \mathbf{p}_1)\cdot\mathbf{r}]U(\mathbf{r})$ can be regarded as the potential scattering between two plane waves [31].

III. HATI SPECTRUM FOR AN *A-B-A* TRIATOMIC MODEL MOLECULE

We now consider a HATI process for a linear *A-B-A* triatomic molecule. We employ a short-range model potential; that is, for an atomic ion of charge c, the potential is of type $c\exp(-r)/r$. The *A-B-A* three-center binding potential of a triatomic molecular ion can thus be written as

$$\begin{aligned} U(\mathbf{r}) = &-c_1\frac{\exp(-|\mathbf{r}-\mathbf{R}_1|)}{|\mathbf{r}-\mathbf{R}_1|} - c_2\frac{\exp(-r)}{r} \\ &- c_1\frac{\exp(-|\mathbf{r}+\mathbf{R}_1|)}{|\mathbf{r}+\mathbf{R}_1|}, \end{aligned} \tag{8}$$

where the origin is located at nucleus B, $\mathbf{r}$ is the position vector of the ionized electron, $\mathbf{R}_1$ and $-\mathbf{R}_1$ are the position vectors of two nuclei A, and c_1 and c_2 are the charges of A and B, respectively.

Using the potential in Eq. (8), the three-center transition amplitude is

$$\langle\mathbf{p}_f|U|\mathbf{p}_1\rangle \propto \frac{4\pi}{1+\Delta p^2}[c_1e^{-i\Delta\mathbf{p}\cdot\mathbf{R}_1} + c_2 + c_1e^{i\Delta\mathbf{p}\cdot\mathbf{R}_1}], \tag{9}$$

where $\Delta\mathbf{p} = \mathbf{p}_f - \mathbf{p}_1$. Equation (9) indicates that the interference pattern of the HATI spectrum is determined not only by the geometric structure of the molecule, that is, the positions of nuclei, but also by the charges carried by each nuclei. Especially, from Eq. (9) one can see that the interference pattern changes with the values of c_1 and c_2: (1) When $c_1 \ll c_2$, the positive charge is carried mainly by atom B and the rescattering electron can only feel an attractive force

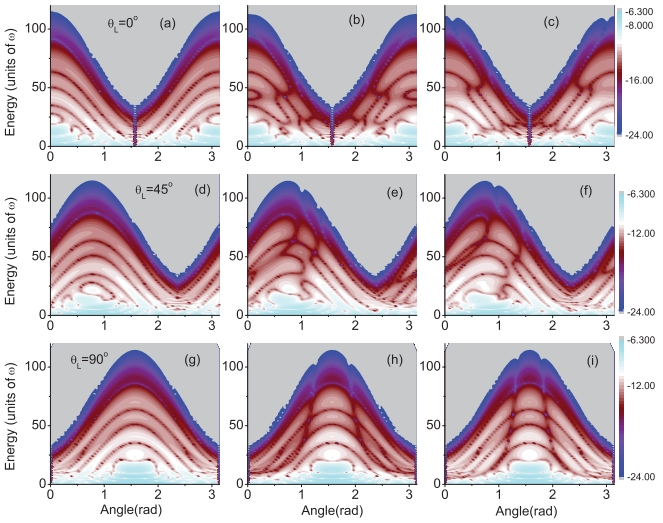

FIG. 1. (Color online) Angle-resolved HATI spectra for an A-B-A model molecule with $R_0 = 2$; the angle between the molecular axis and the laser's electric field is $\theta_L = 0$ (a–c), 45° (d–f), and 90° (g–i). The charge values of A and B are 0.1 and 0.8 (a, d, g), 0.33 and 0.33 (b, e, h), and 0.5 and 0 (c, f, i), respectively.

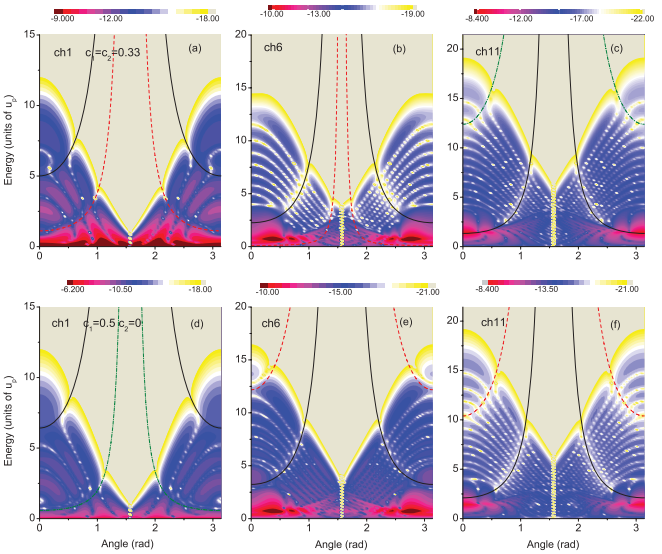

FIG. 2. (Color online) Angle-resolved HATI spectra of an A-B-A model molecule with $R_0 = 2$ and charge values $c_1 = c_2 = 0.33$ (a–c) and $c_1 = 0.5$, $c_2 = 0$ (d–f) for ATI channel 1 (a, d), channel 6 (b, e), and channel 11 (c, f). (a–c) The solid line satisfies $\Delta\mathbf{p}\cdot\mathbf{R}_1 = \frac{4\pi}{3}$, the dashed line satisfies $\Delta\mathbf{p}\cdot\mathbf{R}_1 = \frac{2\pi}{3}$, and the dot-dashed line satisfies $\Delta\mathbf{p}\cdot\mathbf{R}_1 = \frac{8\pi}{3}$. (d–f) The solid line satisfies $\Delta\mathbf{p}\cdot\mathbf{R}_1 = \frac{3\pi}{2}$, the dashed line satisfies $\Delta\mathbf{p}\cdot\mathbf{R}_1 = \frac{5\pi}{2}$, and the dot-dashed line satisfies $\Delta\mathbf{p}\cdot\mathbf{R}_1 = \frac{\pi}{2}$.

from B. Thus the interference fringes on HATI spectrum are similar to those of a single atom. (2) While $c_1 \simeq c_2$, the rescattering electron can feel a three-center attractive force and hence the spectrum can reveal a three-center structure of the molecule. (3) While $c_1 \gg c_2$, the rescattering electron can feel a two-center attractive force and thus the spectrum should show a two-center structure.

To demonstrate the preceding observations, we calculate the HATI spectrum of an A-B-A triatomic model molecule with different values of c_1 and c_2. To simplify the calculation, we use the same value of the ionization threshold and the same wave function for different charge distribution cases. In our calculation, the frequency of the laser field is 0.057 and the intensity is 1.8×10^{14} W/cm^2. Figure 1 presents the angle-resolved HATI spectrum of the triatomic molecule with different charge distributions and θ_L, the angle formed by the molecular axis and the laser's electric field. The figure shows that the interference pattern changes dramatically with c_1 and c_2. From Fig. 1, we can see that, although the molecule is the same, the HATI spectrum can be very different for different charge distributions of its ion. Hence it would be difficult to image the real geometric structure of a molecule by the HATI spectrum without knowing exactly the charge distribution of the corresponding molecular ion.

To investigate the interference pattern of a two-center or three-center recollision process in the HATI spectrum shown in Fig. 1, let us analyze Eq. (9) to extract the interference functions that determine destructive interference fringes. From Eq. (9) we can see that the condition $c_1 \simeq c_2$ corresponds to a three-center recollision process, and the destructive interference pattern in the HATI spectrum fulfills the condition $1 + 2\cos(\Delta\mathbf{p}\cdot\mathbf{R}_1) = 0$, that is,

$$\Delta\mathbf{p}\cdot\mathbf{R}_1 = \frac{2\pi}{3} + 2n\pi, \tag{10}$$

or

$$\Delta\mathbf{p}\cdot\mathbf{R}_1 = \frac{4\pi}{3} + 2n\pi. \tag{11}$$

In contrast, when $c_1 \gg c_2$, which corresponds to a two-center recollision process, the destructive interference curves can be predicted by Eq. (9):

$$\Delta\mathbf{p}\cdot\mathbf{R}_1 = \pi/2 + n\pi. \tag{12}$$

One should note that the preceding equations for predicting the destructive interference by electron recollision in the HATI spectrum are obtained for each ATI channel, where the value of $\Delta\mathbf{p}$ in the direction of the molecular axis is $p_f\cos\theta_f - p_1\cos\theta_1$, with θ_1 being the angle between the momentum $\mathbf{p}_1$ and the molecular axis. Figure 2 presents HATI spectra with $c_1 = c_2 = 0.33$ [Figs. 2(a)–2(c)] and $c_1 = 0.5$, $c_2 = 0$ [Figs. 2(d)–2(f)] for the first ATI channel [Figs. 2(a) and 2(d)], the sixth ATI channel [Figs. 2(b) and 2(e)], and the eleventh ATI channel [Figs. 2(c) and 2(f)]. The lines in Fig. 2 were obtained by Eqs. (10)–(12), which agree well with quantum calculation. The values of momenta p_1 for these lines are $p_1 = 0.11$, 0.76, and 1.07 for the first, sixth, and eleventh channel, respectively. In Figs. 2(a)–2(c), the solid line satisfies $\Delta\mathbf{p}\cdot\mathbf{R}_1 = \frac{4\pi}{3}$, the dashed line satisfies $\Delta\mathbf{p}\cdot\mathbf{R}_1 = \frac{2\pi}{3}$, and the dot-dashed line satisfies $\Delta\mathbf{p}\cdot\mathbf{R}_1 = \frac{8\pi}{3}$. Similarly, in Figs. 2(d)–2(f), the solid line satisfies $\Delta\mathbf{p}\cdot\mathbf{R}_1 = \frac{3\pi}{2}$, the dashed line satisfies $\Delta\mathbf{p}\cdot\mathbf{R}_1 = \frac{5\pi}{2}$, and the dot-dashed line satisfies $\Delta\mathbf{p}\cdot\mathbf{R}_1 = \frac{\pi}{2}$.

From the preceding results, one may find that the destructive interference fringes on an angle-resolved HATI spectrum for each ATI channel can be precisely predicted by the corresponding formula obtained. However, such a formula

does not exist for the total angle-resolved HATI spectrum shown in Fig. 1, because the interference curves shift with ATI channel and the final spectrum is obtained by summing up coherently the spectra of all ATI channels. This difficulty can be partly resolved by applying a low-U_p laser field so that the total HATI yield is mainly contributed from the first few ATI channels, where the shift of interference fringes is small; the result is that the fringes in the total HATI spectrum can be determined approximately by the predicting formulas for the first ATI channels [21].

Based on the results for a triatomic molecule, we can obtain a more general formula for each ATI channel for a polyatomic molecule. Especially, for a complex molecule formed by N atoms, if the potential of the corresponding molecular ion can be modeled by

$$U(\mathbf{r}) = -\sum_{i=1}^{N} c_i \frac{\exp(-|\mathbf{r}-\mathbf{R}_i|)}{|\mathbf{r}-\mathbf{R}_i|}, \tag{13}$$

where c_i is the charge of the ith nucleus and $\mathbf{R}_i$ is its position vector, the destructive interference fringes by multicenter recollision obey the following condition:

$$\sum_{i=1}^{N} c_i \exp(-i\,\Delta\mathbf{p}\cdot\mathbf{R}_i) = 0. \tag{14}$$

From Eq. (14), one may find that the interference pattern caused by multicenter recollision in a HATI spectrum depends on both the charge and the position of each nuclei in the molecular ion.

IV. COMPARISONS OF HATI SPECTRA FOR DIFFERENT MOLECULES

To illustrate the charge distribution effect, we compare the angle-resolved HATI spectrum of CO_2 with that O_2 and the spectrum of NO_2 with that N_2. In our calculations, the laser frequencies are $\omega = 0.028$ and $U_p/\omega = 14$. Under these laser conditions, it is reasonable to assume that the rearrangement of charge distribution of a molecular ion is much faster than the laser cycle after the electron is ionized; thus a stable charge distribution of the molecular ion should appear before the ionized electron is driven back by the laser. Table I reports the charge distributions of the molecular ions CO_2^+ and NO_2^+. One can see from the table that, for CO_2^+ the charge distributions of the ground and the first excited states, where C carries a dominating positive charge (i.e., the charge value of C is >0.5), are similar, which indicates that the charge distribution is mainly determined by the characteristic of individual atoms rather than the state of the molecular ion. Table I shows that atom C dominates the positive charge in

TABLE I. Charge distributions of molecular ions.

CO_2^+ ground state	C	O	O
Charge value	0.75 179	0.12 410	0.12 410
CO_2^+ first excited state	C	O	O
Charge value	1.07 249	−0.036 246	−0.036 246
NO_2^+ ground state	N	O	O
Charge value	0.643 922	0.178 039	0.178 039

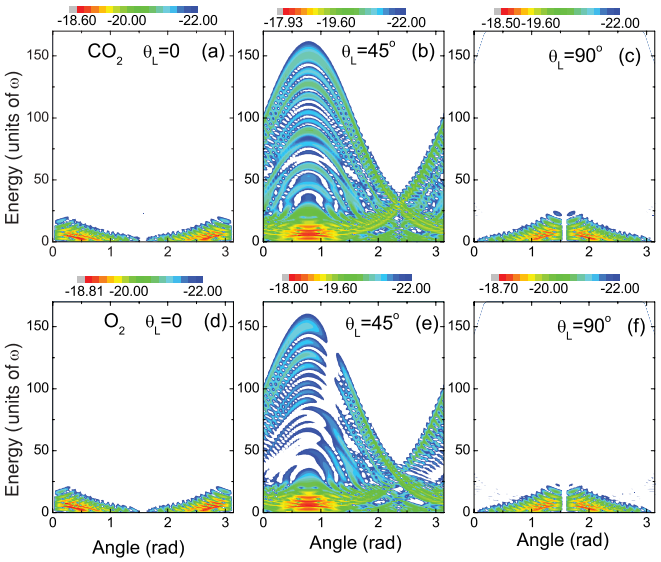

FIG. 3. (Color online) Angle-resolved HATI spectra of CO_2 (a–c) and O_2 (d–f) with angle $\theta_L = 0$ (a, d), 45° (b, d), and 90° (c, f).

CO_2^+, and similarly, atom N dominates the positive charge in NO_2^+. The initial wave functions of CO_2, O_2, NO_2, and N_2 were generated by the GAMESS software [32] at the corresponding equilibrium distances of these molecules. We determine the values c_1 and c_2 for molecular ions CO_2^+ and NO_2^+ from the GAMESS calculation and then use Eq. (8). For linear molecules, the molecular axes of CO_2, O_2, and N_2 are fixed along the z axis, while for the nonlinear molecule NO_2, the two O atoms are located on the z axis, and the N atom is fixed on the x axis. We also assumed that the electric field of the laser rotates in the xz plane at an angle θ_L. The ionized electron was assumed to be emitted in the xz plane at an angle θ_f formed by its momentum and the z axis.

Figure 3 presents the angle-resolved HATI spectra of CO_2 [Figs. 3(a)–3(c)] and O_2 [Figs. 3(d)–3(f)], with $\theta_L = 0$ [Figs. 3(a) and 3(d)], 45° [Figs. 3(b) and 3(e)], and 90° [Figs. 3(c) and 3(f)]. Since the ground states of CO_2 and O_2 are very similar, it is not surprised that the general characteristics of the HATI spectra for these two molecules are very similar, as shown in Fig. 3 for different molecular orientations. Especially, when $\theta_L = 0$ and 90°, there are no HATI spectra because of π_g symmetry of their initial wave functions, which agree well with the results in [28]. However, for the case of $\theta_L = 45°$, one can find the difference in the spectra for CO_2 and O_2: destructive interference curves caused by two-center recollision are present in the spectrum of O_2, while these interference curves completely disappear for CO_2. This difference between their HATI spectra can be attributed mainly to the difference in the charge distributions of their corresponding molecular ions. As reported in Table I, the positive charge of CO_2^+ is mainly carried by atom C and thus the returning electron is more attracted by C when it recollides with CO_2^+; the result is that the recollision process for the returning electron is dominated by a single-center rescattering process.

To compare the case of N_2 and NO_2, we present in Fig. 4 the angle-resolved HATI spectra of NO_2 [Figs. 4(a)–4(c)]

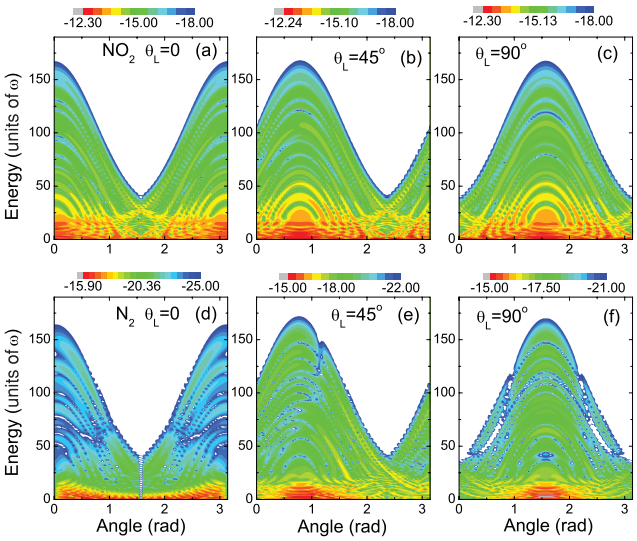

FIG. 4. (Color online) Angle-resolved HATI spectra of NO_2 (a–c) and N_2 (d–f) with the emitted electron in the molecule-laser plane and $\theta_L = 0$ (a, d), 45° (b, e), and 90° (c, f).

and N_2 [Figs. 4(d)–4(f)] with different molecular orientations, $\theta_L = 0$ [Figs. 4(a) and 4(d)], 45° [Figs. 4(b) and 4(e)], and 90° [Figs. 4(c) and 4(f)]. It is shown that the HATI spectra for all θ_L cases have the cutoff of $10U_p$ along the laser's electric field. The difference between the NO_2 and the N_2 spectra is clear: destructive interference curves caused by the two-center recollision are present for N_2 in Figs. 4(d)–4(f), while there are no such interference curves for NO_2, as shown in Figs. 4(a)–4(c), because of the single-center recollision process for NO_2, which is similar to the case for CO_2.

The foregoing results have confirmed our prediction: with the charge distributions of CO_2^+ and NO_2^+ given in Table I, the geometric structures of CO_2 and NO_2 cannot be imaged by using the destructive interference fringes in the angle-resolved HATI spectra even if one can align these molecules along the direction of the laser's electric field; this is because the dominating process is a single-center recollision for CO_2 and NO_2. In contrast, the geometric structures of O_2 and N_2 can be well imaged by the destructive interference of two-center recollision trajectories in HATI spectra at a suitable alignment angle, as shown in Figs. 3(e), 4(d) and 4(e).

V. CONCLUSIONS

In summary, we have investigated the angle-resolved HATI spectra of *A*-*B*-*A* triatomic molecules using frequency-domain theory. The dependence of a HATI spectrum on the charge distribution in a molecular ion as seen by the recolliding electron has been studied. We have found that the interference pattern of a molecular structure in a HATI spectrum varies dramatically with the charge distribution. Thus the charge distribution of a molecular ion is a crucial factor for imaging molecular geometry structure. On the other hand, an angle-resolved HATI spectrum can be used as a very powerful tool for investigating the dynamic process of a complex molecule interacting with a laser field.

ACKNOWLEDGMENTS

This research was supported by the National Natural Science Foundation of China under Grants No. 60778009 and 60708003 and by 973 Research Project No. 2006CB806003. Z.C.Y. was supported by the NSERC of Canada and by the Canadian computing facilities ACEnet, SHARCnet, and WestGrid. B.W. thanks Jing Chen and Jiangbin Gong for helpful discussions and suggestions.

[1] D. Shafir, Y. Mairesse, D. M. Villeneuve, P. B. Corkum, and N. Dudovich, Nature Phys. **5**, 412 (2009).
[2] A. Cerkic, E. Hasovic, D. B. Milosevic, and W. Becker, Phys. Rev. A **79**, 033413 (2009).
[3] H. J. Worner, H. Niikura, J. B. Bertrand, P. B. Corkum, and D. M. Villeneuve, Phys. Rev. Lett. **102**, 103901 (2009).
[4] M. Okunishi, T. Morishita, G. Prumper, K. Shimada, C. D. Lin, S. Watanabe, and K. Ueda, Phys. Rev. Lett. **100**, 143001 (2008).
[5] T. Zuo, A. D. Bandrauk, and P. B. Corkum, Chem. Phys. Lett. **259**, 313 (1996).
[6] M. Lein, N. Hay, R. Velotta, J. P. Marangos, and P. L. Knight, Phys. Rev. Lett. **88**, 183903 (2002).
[7] J. Itatani, J. Levesque, D. Zeidler, Hiromichi Niikura, H. Pepin, J. C. Kieffer, P. B. Corkum, and D. M. Villeneuve, Nature (London) **432**, 867 (2004).
[8] H. Hetzheim, C. Figueira de Morisson Faria, and W. Becker, Phys. Rev. A **76**, 023418 (2007).
[9] A.-T. Le, X.-M. Tong, and C. D. Lin, Phys. Rev. A **73**, 041402(R) (2006); V. Le, N.-T. Nguyen, C. Jin, A.-T. Le, and C. D. Lin, J. Phys. B: At. Mol. Opt. Phys. **41**, 085603 (2008).
[10] S. Micheau, Z. Chen, A. T. Le, J. Rauschenberger, M. F. Kling, and C. D. Lin, Phys. Rev. Lett. **102**, 073001 (2009).
[11] M. Kitzler, X. Xie, S. Roither, A. Scrinzi, and A. Baltuska, New J. Phys. **10**, 025029 (2008).
[12] M. Meckel, D. Comtois, D. Zeidler, A. Staudte, D. Pavicic, H. C. Bandulet, H. Pepin, J. C. Kieffer, R. Dorner, D. M. Villeneuve, and P. B. Corkum, Science **320**, 1478 (2008).
[13] A. A. Gonoskov, I. A. Gonoskov, M. Yu. Ryabikin, and A. M. Sergeev, Phys. Rev. A **77**, 033424 (2008).
[14] O. Smirnova, Y. Mairesse, S. Patchkovskii, N. Dudovich, D. Villeneuve, P. Corkum, and M. Yu. Ivanov, Nature (London) **460**, 972 (2009).
[15] F. Krausz and M. Ivanov, Rev. Mod. Phys. **81**, 163 (2009).
[16] P. B. Corkum, Phys. Rev. Lett. **71**, 1994 (1993); K. C. Kulander, K. J. Schafer, and J. L. Krause, in *Super Intense Laser-Atom Physics*, edited by K. Rzazewski (Plenum, New York, 1993), Vol. 316, p. 95.
[17] D. Guo and T. Åerg, J. Phys. A **21**, 4577 (1988); D. Guo and G. W. F. Drake, *ibid.* **25**, 3383 (1992); D.-S. Guo, T. Åerg, and B. Crasemann, Phys. Rev. A **40**, 4997 (1989).
[18] L. Gao, X. Li, P. Fu, R. R. Freeman, and D. S. Guo, Phys. Rev. A **61**, 063407 (2000).
[19] P. Fu, B. Wang, X. Li, and L. Gao, Phys. Rev. A **64**, 063401 (2001).

[20] B. Wang, L. Gao, X. Li, D. S. Guo, and P. Fu, Phys. Rev. A **75**, 063419 (2007).
[21] Y. Guo, P. Fu, Z.-C. Yan, J. Gong, and B. Wang, Phys. Rev. A **80**, 063408 (2009).
[22] H. Kang *et al.*, Phys. Rev. Lett. **104**, 203001 (2010).
[23] M. Lein, J. P. Marangos, and P. L. Knight, Phys. Rev. A **66**, 051404 (2002).
[24] M. Spanner, O. Smirnova, P. B. Corkum, and M. Y. Ivanov, J. Phys. B **37**, L243 (2004).
[25] S. N. Yurchenko, S. Patchkovskii, I. V. Litvinyuk, P. B. Corkum, and G. L. Yudin, Phys. Rev. Lett. **93**, 223003 (2004).
[26] D. B. Milosevic, Phys. Rev. A **74**, 063404 (2006).
[27] M. Busuladzic, A. Gazibegovic-Busuladzic, D. B. Milosevic, and W. Becker, Phys. Rev. A **78**, 033412 (2008).
[28] M. Busuladzic, A. Gazibegovic-Busuladzic, and D. B. Milosevic, Phys. Rev. A **80**, 013420 (2009).
[29] M. Okunishi, R. Itaya, K. Shimada, G. Prumper, K. Ueda, M. Busuladzic, A. Gazibegovic-Busuladzic, D. B. Milosevic, and W. Becker, Phys. Rev. Lett. **103**, 043001 (2009).
[30] H. R. Reiss, Phys. Rev. A **22**, 1786 (1980).
[31] Our frequency-domain theory is a theory in velocity gauge, hence the collision matrix elements depend on P_f, rather than the mechanical momentum at the time of scattering. However, we found that our final results agree well qualitatively with the results by Busuladzic *et al.* in [27] (in length gauge). And we believe that the main conclusion of this work will not be affected by the gauge of the theory.
[32] A. A. Granovsky, PC-GAMESS [http://classic.chem.msu.su/gran/gamess/index.html].